Monte Carlo simulation of linear accelerator Varian Clinac iX

E Hedin, A Bäck, J Swanpalmer and R Chakarova
Sahlgrenska University Hospital, Gothenburg, Sweden

Excerpt of report MFT-Radfys 2010:01

Contact: roumiana.chakarova@vgregion.se

1 Introduction

This document presents methods and results from the development of a Monte Carlo model of a Varian Clinac iX linear accelerator of nominal energy 6 MV. It is an excerpt of Report MFT-Radfys 2010:01 at the University of Gothenburg and Sahlgrenska University Hospital in Gothenburg. The simulations were made by the BEAMnrc/EGSnrc Monte Carlo code package [1]. The work presented includes adjusting a model for open fields and does not consider MLC component or wedges.

The aim of the document was to describe how model parameters have been optimised and how the quality of the model has been verified. The parameters adjusted in the model were the energy of the electrons (monoenergetic) incident (normally) on the target as well as the width of the spatial distribution of the electrons (assumed to be Gaussian). The accelerator head was simulated in one step and the dose distribution in water was calculated in a subsequent step. Simulated data were compared to measured data visually, quantatively by directly comparing the numbers and by statistically weighting the differences in a chi^2/NDF analysis.

2 Material/methods

A virtual model of the linear accelerator Varian Clinac iX was built in BEAMnrc (Graphical User Interface 2.0) based on technical data provided by Varian Medical Systems. The calculations were made partly on a local computer with an Intel Core-2 Duo processor (1066MHz FSB, 4MB L2) using Ubuntu operating system and partly on a Linux cluster on the National Supercomputer Centre (NSC), Linköping, Sweden (operating system CentOS 5 x86_64 and Intel Xeon E5345 processors). On NSC the program was run in a parallell mode, using several processors for each job.

2.1 Accelerator head simulation in BEAMnrc

The global photon and electron cut-off energy was 0.01 MeV and 0.7 MeV respectively. The variance reduction technique directional bremsstrahlung (DBS) was used. DBS-splitting field

radius as well as field size was defined at a distance 100 cm from the top of the target. When varying the parameters, the field sizes 10x10 and 20x20 cm^2 were simulated with DBS-radius 15 cm and field sizes 30x30 and 40x40 cm^2 were simulated with DBS-radius 21 cm and 30 cm, respectively. In the stage of verifying the optimum parameter set, field size 2x2 cm^2 was simulated with DBS-radius 10 cm, field sizes 4x4 and 10x10 cm^2 were simulated with DBS radius 20 cm and field sizes 20x20 and 40x40 cm^2 were simulated with DBS radius 30 cm. The splitting number was set to 1000 and the electron splitting was performed in the lower layers of the flattening filter as recommended in the BEAMnrc users manual [1]. Range rejection was turned on with varying ECUTRR (= the minimum energy a charged particle needs to be able to reach the bottom of the accelerator and still having more than 0.7 MeV). Range rejection was considered for electrons with energy less than 2 MeV (ESAVE_GLOBAL = 2) except for in the target where range rejection was considered for electrons with energy less than 1 MeV. Such range rejection run parameters have for example been used by Hasenbalg *et. al.* [2].

Source number 19 (Parallel circular beam with gaussian radial distribution) was used in the production of phase-space files. The electron beam was assumed to be monoenergetic and the two parameters varied to fit the model to measurements were the electron energy and the width of the electron beam hitting the target. The width of the gaussian radial distribution, the focal spot width (FSW), was defined as the Full Width at Half Maximum (FWHM) of the distribution (i.e the width of the distribution where the distribution is half of its maximum value). The electron beam was set to be incident normal to the target surface.

2.2 In-air

A first estimate of the energy of the electrons incident on the target was found by comparing kerma-profiles collected in air for different energies with measured profiles, as described by Sheikh-Bagheri *et. al.* [3]. Water-kerma-profiles were produced by processing the phase-space file in a modified version of beamdp. The weight of each photon is multiplied by its energy, mass-energy-absorption coefficient (Hubbel and Seltzer [4]) and one over the cosine of the angle its direction makes with the z-axis. The measurements were performed, at a distance 100 cm from the top of the target using a cylindrical ionisation chamber (Exradin T2 Spokas Thimble chamber, 0.53 cm^3) with a build-up cap of brass. The dose profiles were normalised to the value at the central axis. The ratio will in the remainder of the text be referred to as the off-axis factor.

2.3 Water Phantom

The dose profiles in water phantom were calculated by the Monte Carlo code DOSXYZnrc. The depth dose-curves were calculated with the CHAMBER module in BEAMnrc. No range rejection was used. The electrons were tracked until their energy was below 0.512 MeV and the photons were tracked until their energy was below 0.010 MeV. The edge of the phantom was kept more than 10 cm away from the field edge and more than 10 cm deeper than the last data point. In the stage of optimising parameters, dose profiles in x-direction (defined by the lower pair of collimators) were analysed. When verifying the model for the field sizes 10x10 and 20x20 cm^2 y-direction (defined by the upper pair of collimators) dose profiles were included. The measurements were performed using thimble ionisation chambers. For field sizes larger than 2x2 cm^2 the CC13 (0.13 cm^2, inner air cavity diameter 0.6 cm) chamber manufactured by Iba Dosimetry was used. For field size 2x2 cm^2 the PTW pin-point (0.015 cm^3, central electrode of steel) chamber was utilized.

The mesaured and simulated dose profiles and depth dose curves were compared visually but also by two different cost functions, namely chi^2/NDF and the number of simulated data points deviating more than a given percentage from the measured profile. The value of chi^2/NDF was calculated according to Equation 1.

$$\chi^2/NDF = \sum_{i=1}^{N} \frac{(s_i - m_i)^2}{\sigma_i^2}/(N-1), \tag{1}$$

where m_i and s_i are the measured and simulated normalised dose values, respectively. σ_i is the standard error of the $i:th$ simulated value and N is the number of data points compared. NDF (Number of Degrees of Freedom) is in this case $N-1$ since σ is estimated using s_i (for more details on how statistics are handled, see the BEAMnrc users manual [1] or B. R. B. Walters *et. al.* [5]).

2.3.1 Dose Profiles

The central voxels of the large fields were 1 cm wide (square top area), the remaining voxels were 0.3 cm wide. In the cases of 4x4 cm^2 and 2x2 cm^2 field sizes the central voxels were 0.5 cm wide and the remaining were 0.5 cm and 0.2 cm wide, respectively. The voxel widths in the cases of 4x4 cm^2 and 2x2 cm^2 field sizes were chosen to correspond to the dimensions of the ionisation chambers to make the simulated penumbral region comparable to the measured.

Pilot simulations were made for a 10x10 cm^2 field when keeping the energy at a value of 6 MeV and varying the FSW from 1 cm to 0.06 cm. Simulations for optimisation of parameters were made for 20x20 and 40x40 cm^2 field sizes. Field size 40x40 cm^2 was simulated for

the following parameter combinations; 5.8 MeV with 0.05 and 0.1 cm FSW as well as 5.7 Mev with 0.08, 0.1 and 0.15 cm FSW. Field size 20x20 cm^2 was simulated for the same parameter combinations except for that no simulation was made using the parameter combination 5.7 MeV and 0.08 cm FSW.

In the stage of varying parameters, dose profiles were extracted at 1.5, 5 and 10 cm depth and the voxels were 0.5 cm deep. With the optimum parameter set chosen, dose profiles were verified at 1.5, 5, 10 and 20 cm depth using voxels that were 0.5, 0.5, 0.5 and 1 cm deep, respectively. The measured dose profiles for 40x40 cm^2 field size were half-profiles. The simulated profiles were in this case averaged over positive and negative x-axis to receive better statistics.

2.3.2 Depth Dose

The depth dose was determined in 0.2 cm high standing cylinders with radius 0.75 cm at the central axis, except for in the case of 2x2 cm^2 field size. In this case the cylinders were 0.3 cm high with radius 0.15 cm.

Pilot simulations were made for a 10x10 cm^2 field keeping the FSW at a value of 0.06 cm and varying the energy in steps of 0.2 MeV from 5.2 MeV to 6.4 MeV. To verify the chosen optimum parameter set, depth dose simulations were performed for field sizes 2x2, 4x4, 10x10, 20x20 and 40x40 cm^2.

2.3.3 Outputfactors

The output factors were defined as the ratio between the dose at the central axis at 10 cm depth, for a given field size, and the dose at central axis at 10 cm depth for a 10x10 cm^2 square reference field. The dose at 10 cm depth was assessed in two different ways; from (i) a fifth grade polynomial fitted to dose values between depth 5 cm and 20 cm and (ii) from the voxel containing the point of interest.

3 Results

3.1 In-air

The statistical uncertainties of the simulations were low. The phase-space-files consisted of around 3.5E8 particles for 20x20 cm^2 field size and between 2E8 and 8E8 particles for 30x30 cm^2 field size. The relative uncertainty (1 sigma) of the simulated values were 0.1% or smaller for each point. Changing the value of FSW from 0.1 to 0.05 cm did not significantly influence the in-air profiles. The simulated off-axis factors for different energies, keeping FSW at 0.05 cm, are presented in the diagrams in Figure 1 together with the measured off-axis-factors. The off-axis distances were 12 cm and 7.5 cm for 30x30 and 20x20 cm^2 field size, respectively. The optimum energy for 0.05 cm FSW was found to be 5.71 and 5.78 MeV for 20x20 and 30x30 cm^2 field size, respectively.

3.2 Water Phantom Simulations

The pilot simulations suggested no change in lateral profiles when going below 0.1 cm FSW for a 10x10 cm^2 field. Regarding depth dose curves, energies between 5.6 and 6.2 MeV could be considered equally good when compromising between good fit at dose-max and good fit at deeper depths (discarding any change in depth dose curve due to FSW).

3.2.1 Dose Profiles

The optimum parameter set was chosen to be; 5.7 MeV energy of the electrons incident on the target and 0.1 cm FSW. Corresponding profiles are shown in Figures 2 to 6. All profiles go through the central axis. The dose has been normalised to the dose at central axis for each depth.

For the parameter set [5.7 MeV 0.1 cm] none of the simulated data points, between x=0 and x=19.75 cm, in Figure 2 a), b), c) and d) deviate from measured data more than 1.5%, 1%, 1% and 1.8% of the central axis dose at the given depth, respectively. The deviation should be considered in conjunction with the relative standard errors of the normalised simulated values, which, within the actual, interval are between 0.3% and 0.4%.

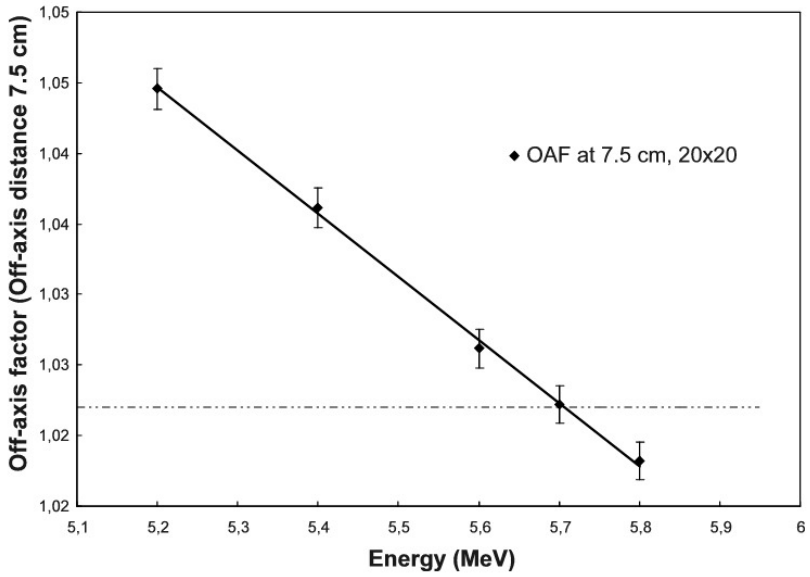

(a)

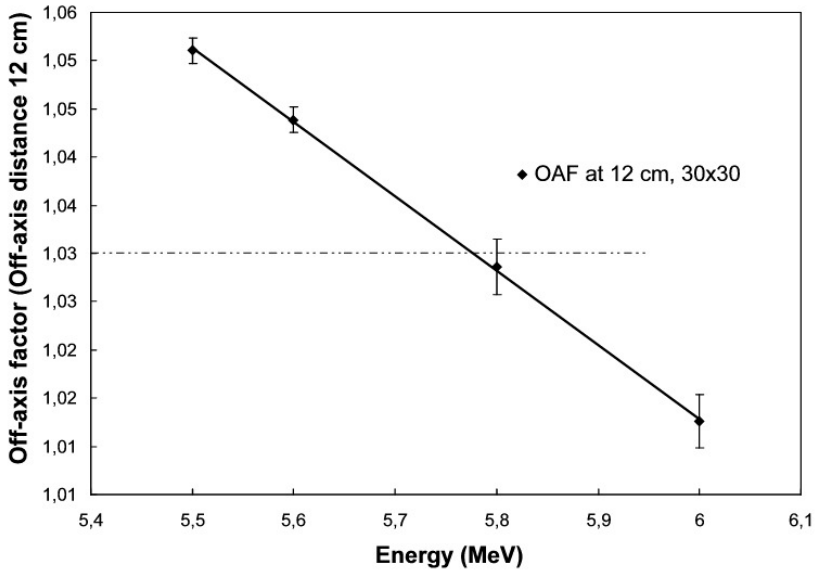

(b)

Figure 1: Off-axis factors (OAF) plotted against the energy of electrons incident on the target for the field sizes (a) 20x20 cm^2 and (b) 30x30 cm^2. The dashed line represents the measured value of off-axis factor at 7.5 cm and 12 cm off axis distance, respectively. The errorbars represent the 95% confidence interval of the simulated data points.

The simulated and measured profiles for 20x20 cm^2 field size for parameter set [5.7 MeV 0.1 cm], are seen in Figure 3. None of the simulated data points between, x=-8.95 and x=8.95 cm in Figure 3 a), b), c) and d) deviate from measured data more than 1.4%, 1%, 1.3% and 1.2% of the central axis dose at the given depth, respectively. The deviation should be considered together with the relative standard errors of the normalised simulated values which, within the actual interval, are between 0.45% and 0.55%.

The chosen parameter set [5.7 MeV 0.1 cm] was further verified for field sizes 10x10, 4x4 and 2x2 cm^2. These profiles are shown in Figures 4 to 6. In the case of 10x10 cm^2 field size none of the simulated data points between x=-4.25 and x=4.25 cm in Figure 4 a), b), c) and d) deviate from measured data more than 1.7%, 1%, 1.5% and 1.2% of the central axis dose at the given depth, respectively. The deviation should be considered in conjunction with the relative standard errors of the normalised simulated values which, within the actual interval, are around 0.4%.

The field sizes 4x4 and 2x2cm^2 were analysed visually and the simulated penumbra was assured to agree with measured data to within 1 mm except for at 1.5 cm depth for the 2x2 cm^2 field and both 1.5 cm and 5 cm depth for the 4x4 cm^2 field, where the difference was between 1 and 1.5 mm. This larger difference was observed at only one of the field edges. It should be noted that the measured fields are not centered.

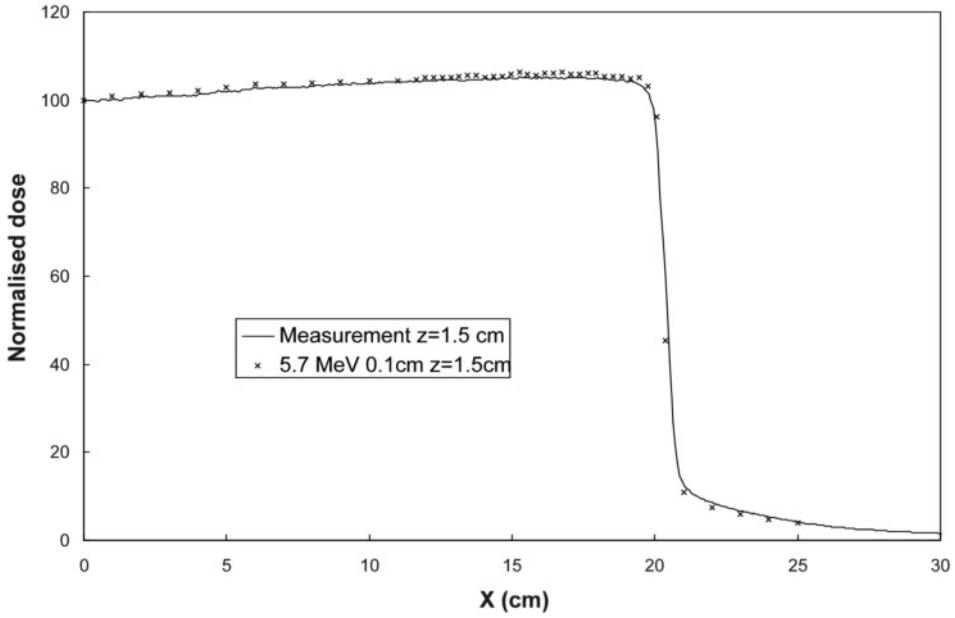
Normalised dose
X (cm)
Measurement z=1.5 cm
5.7 MeV 0.1cm z=1.5cm
0
20
40
60
80
100
120
0
5
10
15
20
25
30

(a)

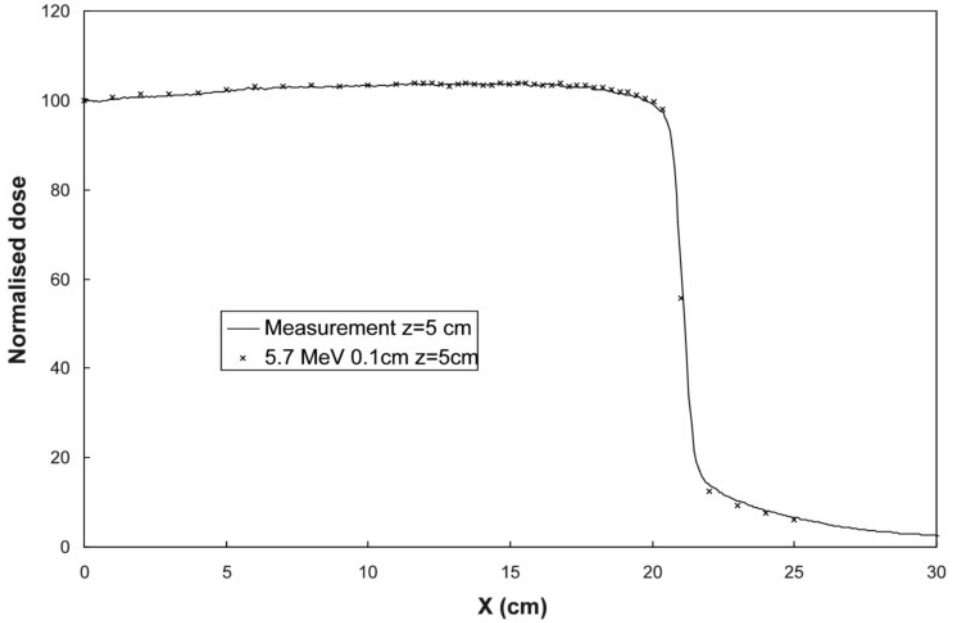
Normalised dose
X (cm)
Measurement z=5 cm
5.7 MeV 0.1cm z=5cm
0
20
40
60
80
100
120
0
5
10
15
20
25
30

(b)

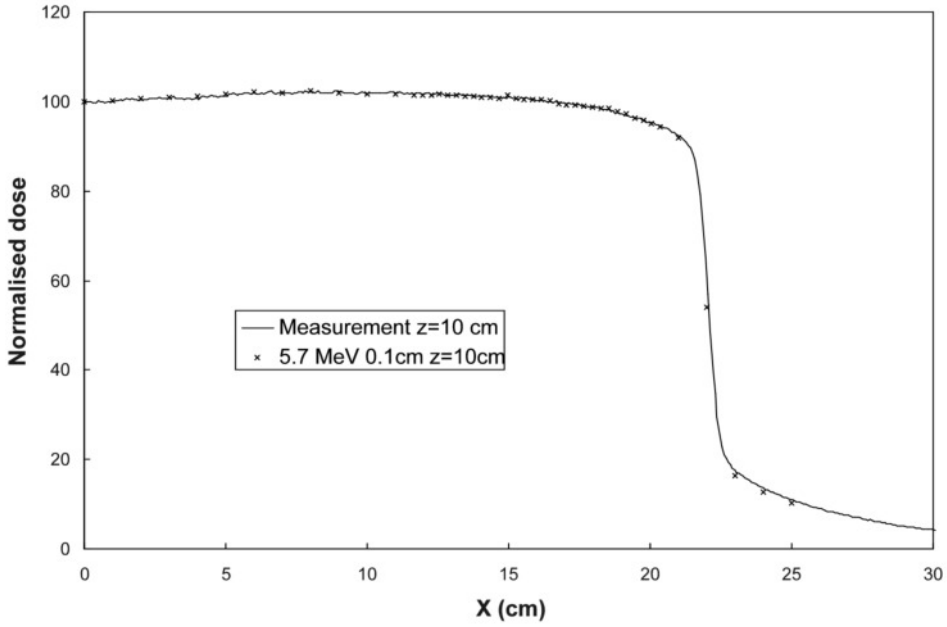

(c)

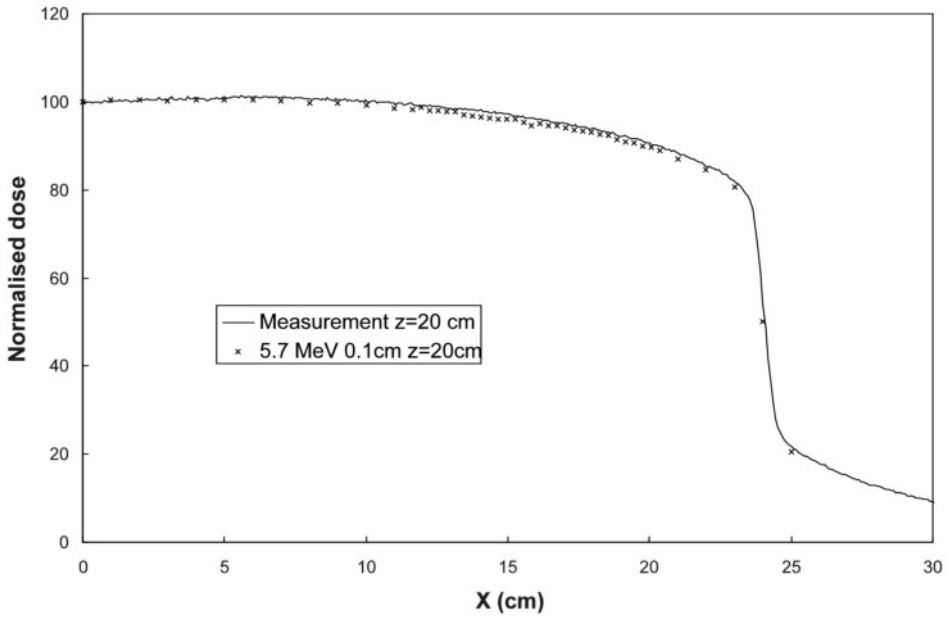

(d)

Figure 2: Dose profile for 40x40 cm^2 field size in water phantom at a) 1.5 cm, b) 5 cm, c) 10 cm, d) 20 cm depth. Solid line measured (CC13) and discrete points simulated. The uncertainties of the simulated values (+-1SE) are represented by the size of the data points. Deviation between measured and simulated data is less than a) 1.5%, b) 1%, c) 1%, d) 1.8% of the dose at central axis in the range x=0 to 19.75 *cm*.

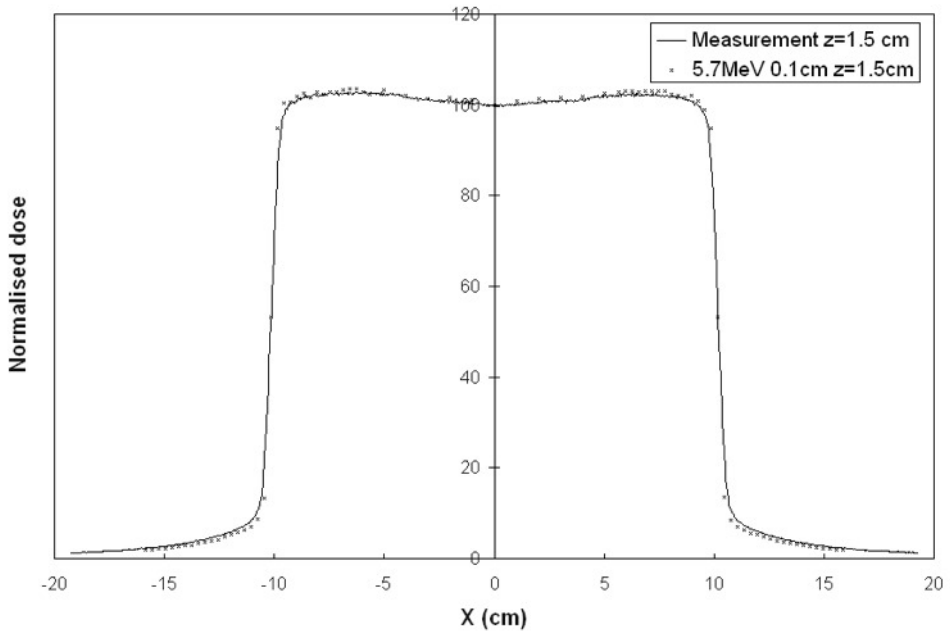
Measurement z=1.5 cm
5.7MeV 0.1cm z=1.5cm
Normalised dose
X (cm)
120
100
80
60
40
20
0
-20
-15
-10
-5
0
5
10
15
20

(a)

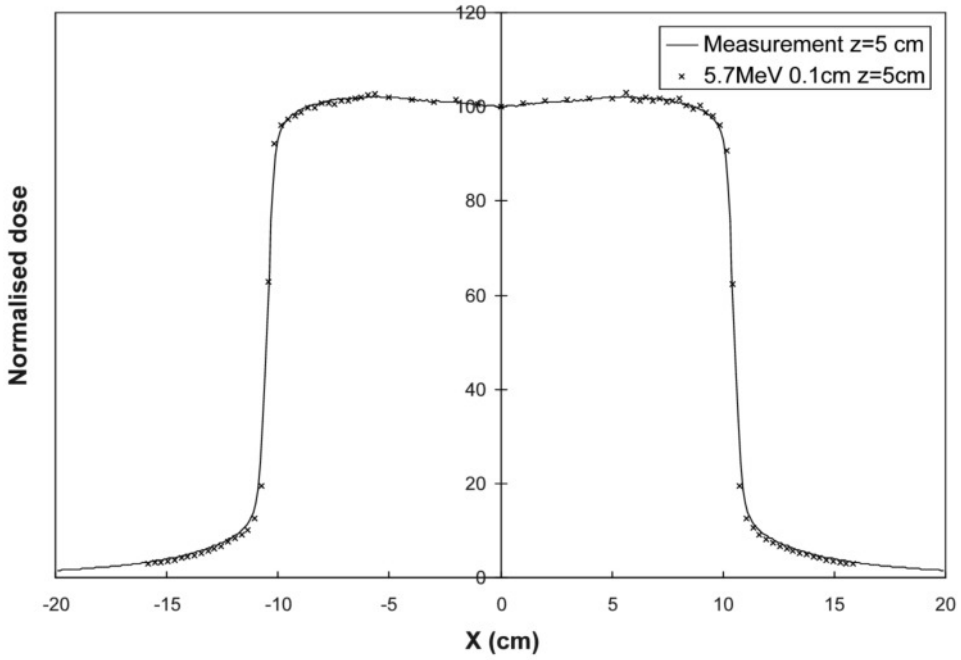
Measurement z=5 cm
5.7MeV 0.1cm z=5cm
Normalised dose
X (cm)
120
100
80
60
40
20
0
-20
-15
-10
-5
0
5
10
15
20

(b)

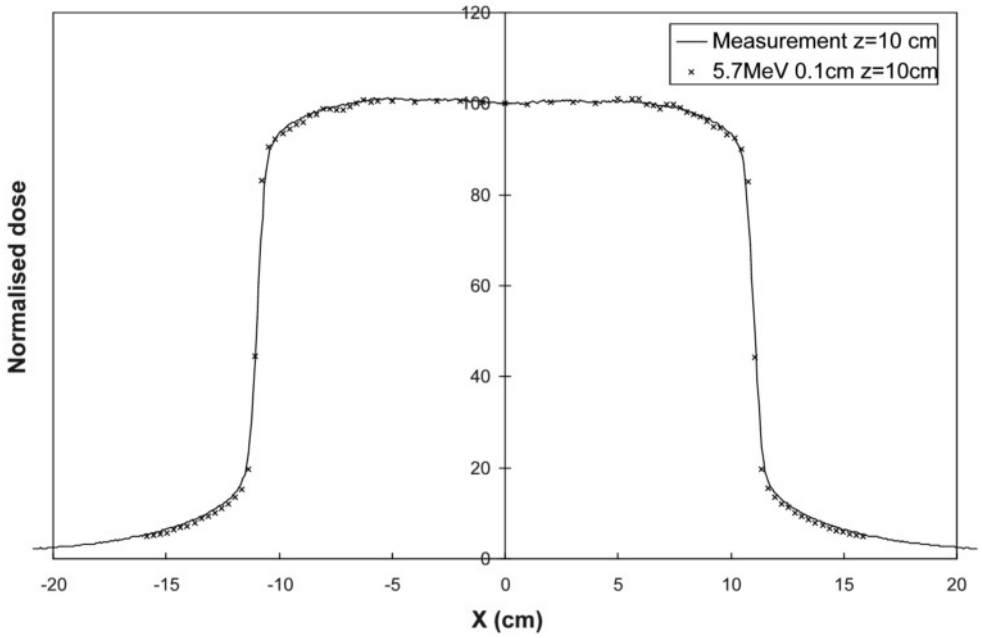

(c)

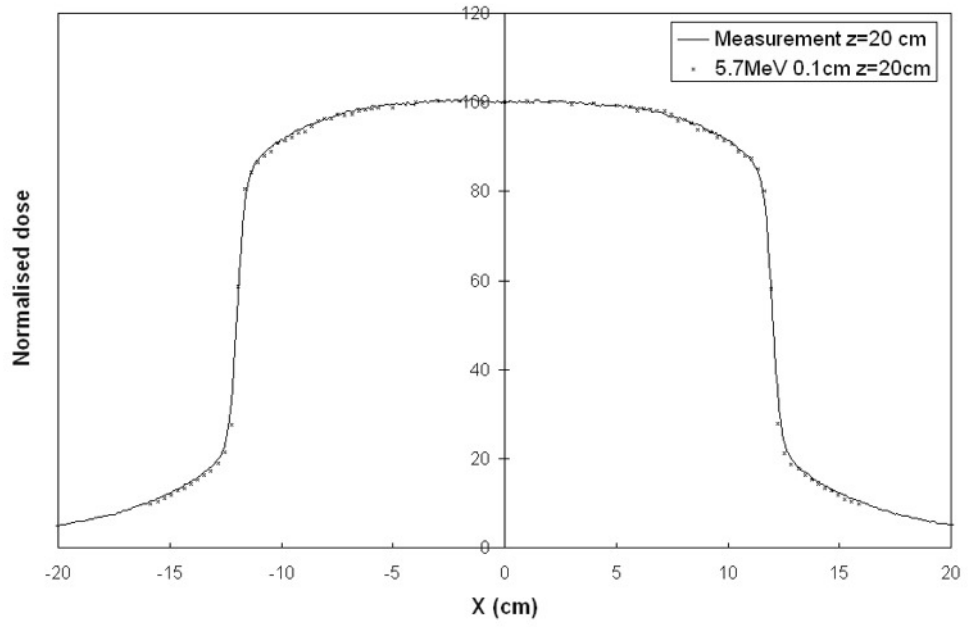

(d)

Figure 3: Dose profile for 20x20 cm^2 field size in water phantom at a) 1.5 cm, b) 5 cm, c) 10 cm, d) 20 cm depth. Solid line measured (CC13) and discrete points simulated. The uncertainties of the simulated values (+-1SE) are represented by the size of the data points. Deviation between measured and simulated data is less than a) 1.4%, b) 1%, c) 1.3%, d) 1.2% of the dose at central axis in the range x=-8.95 to x=8.95 *cm*.

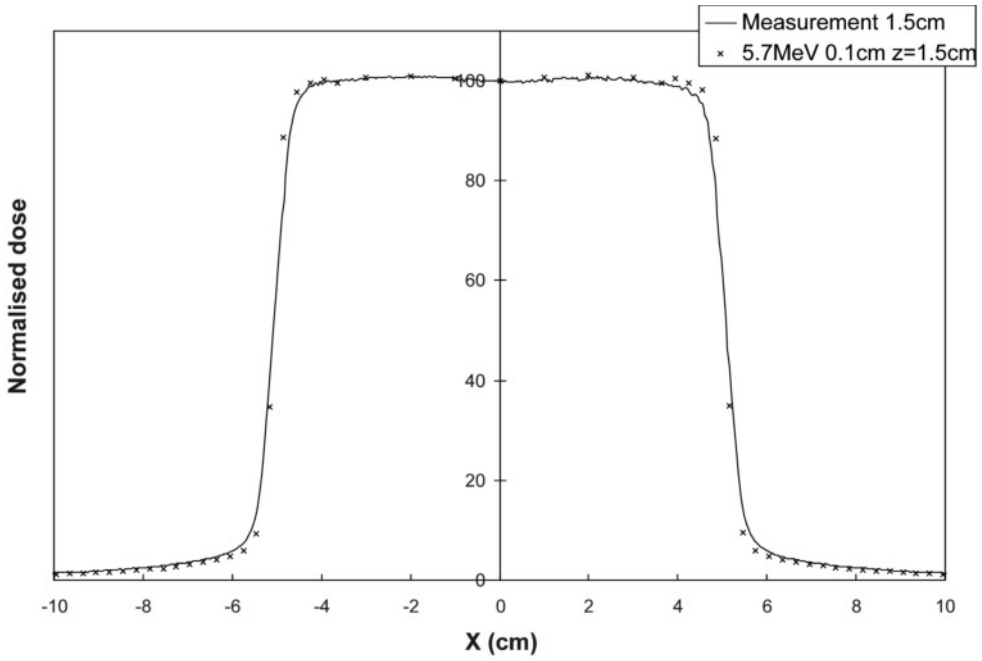
Measurement 1.5cm
5.7MeV 0.1cm z=1.5cm
Normalised dose
X (cm)
0
20
40
60
80
100
-10
-8
-6
-4
-2
0
2
4
6
8
10

(a)

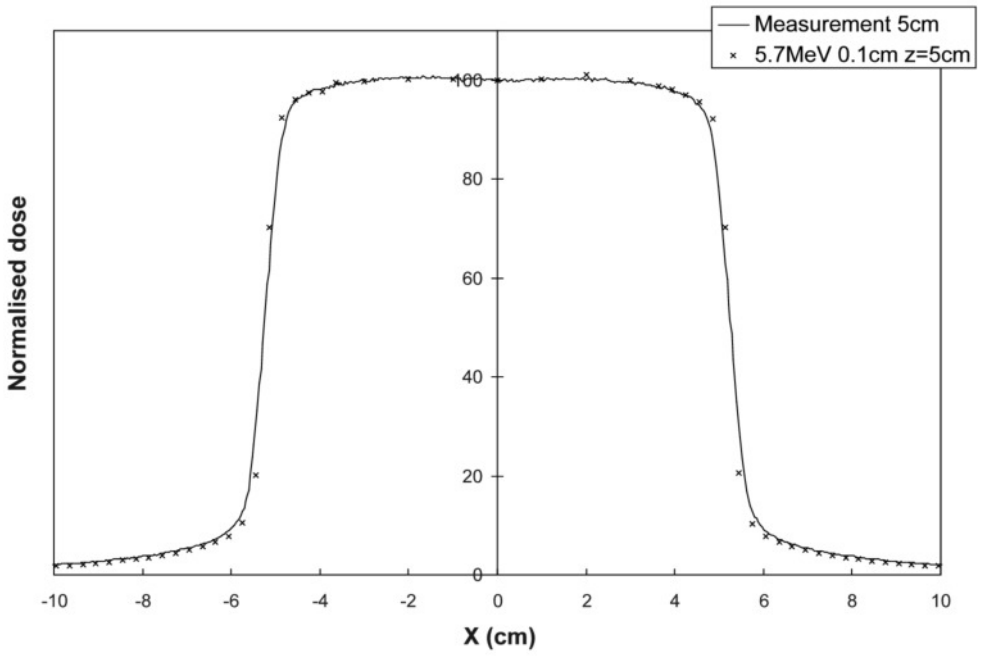
Measurement 5cm
5.7MeV 0.1cm z=5cm
Normalised dose
X (cm)
0
20
40
60
80
100
-10
-8
-6
-4
-2
0
2
4
6
8
10

(b)

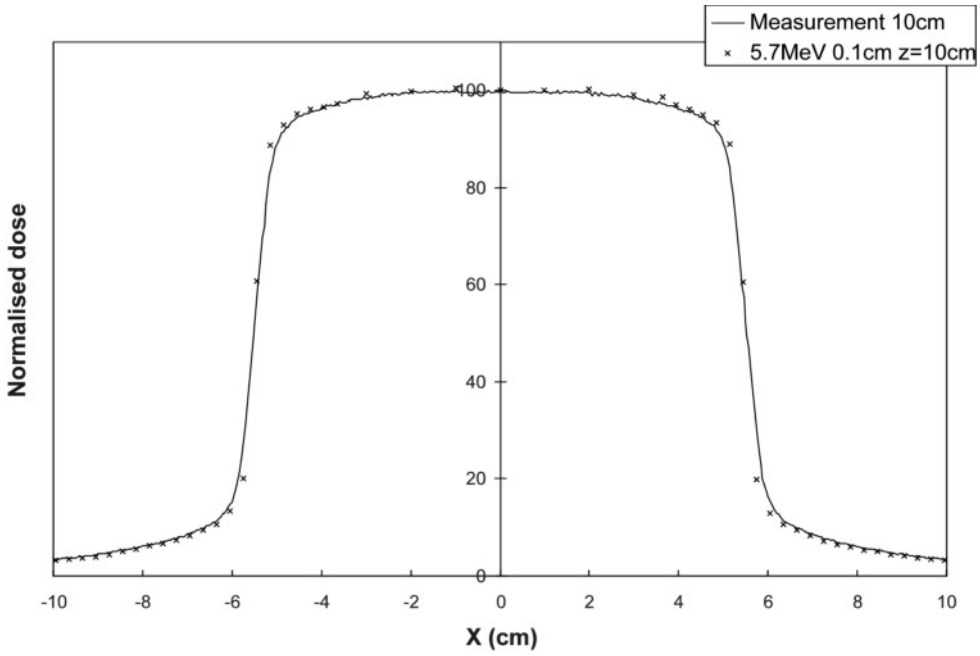

(c)

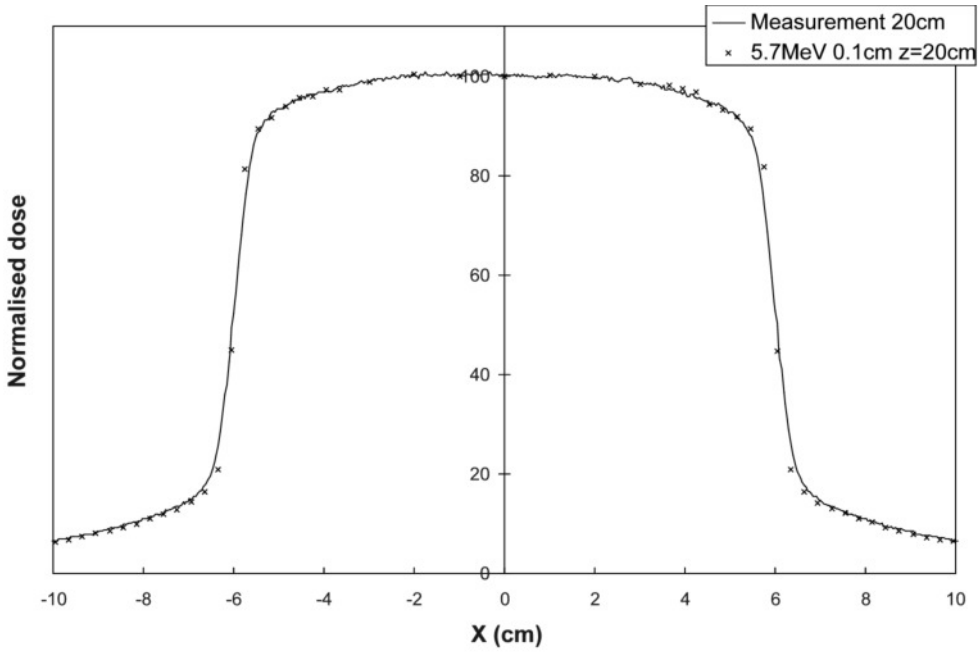

(d)

Figure 4: Dose profile for 10x10 cm^2 field size in water phantom at a) 1.5 cm, b) 5 cm, c) 10 cm, d) 20 cm depth. Solid line measured (CC13) and discrete points simulated. The uncertainties of the simulated values (+-1SE) are represented by the size of the data points. Deviation between measured and simulated data is less than a) 1.7%, b) 1%, c) 1.5%, d) 1.2% of the dose at central axis in the range x=-4.25 to x=4.25 *cm*.

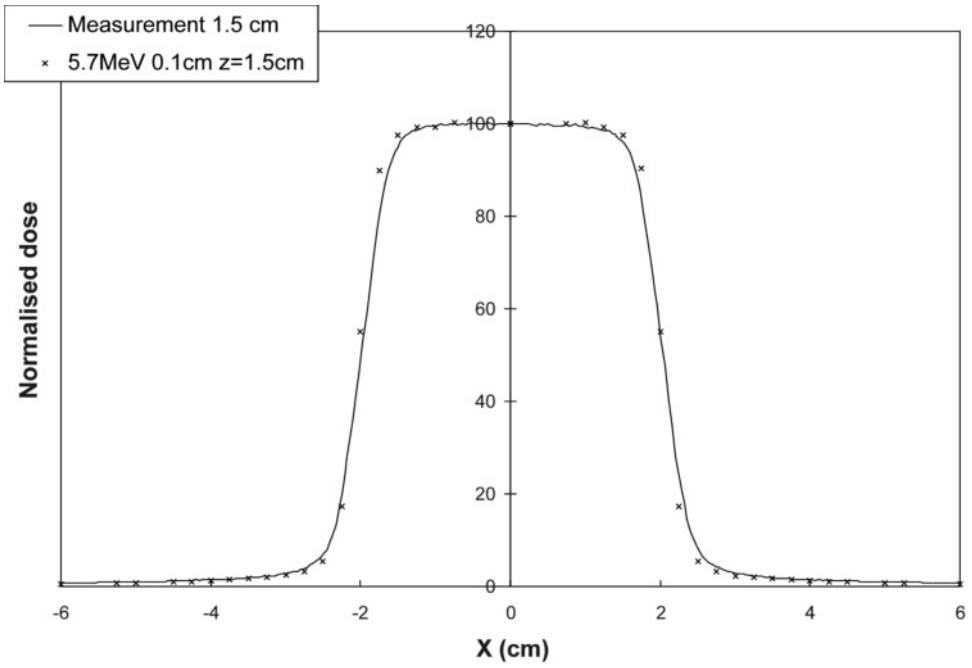
Measurement 1.5 cm
5.7MeV 0.1cm z=1.5cm
Normalised dose
X (cm)
120
100
80
60
40
20
0
-6
-4
-2
0
2
4
6

(a)

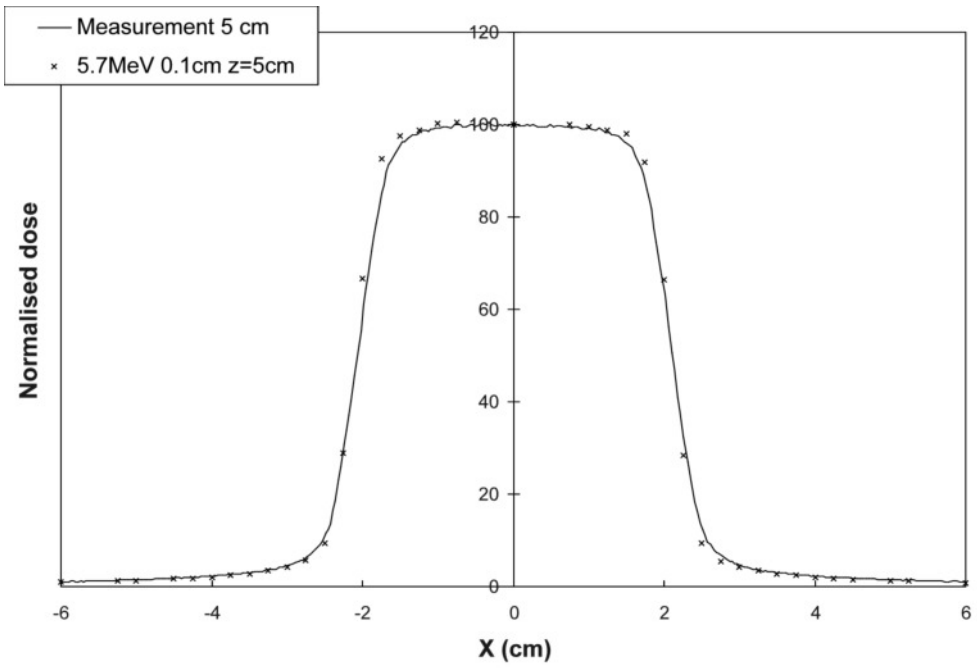
Measurement 5 cm
5.7MeV 0.1cm z=5cm
Normalised dose
X (cm)
120
100
80
60
40
20
0
-6
-4
-2
0
2
4
6

(b)

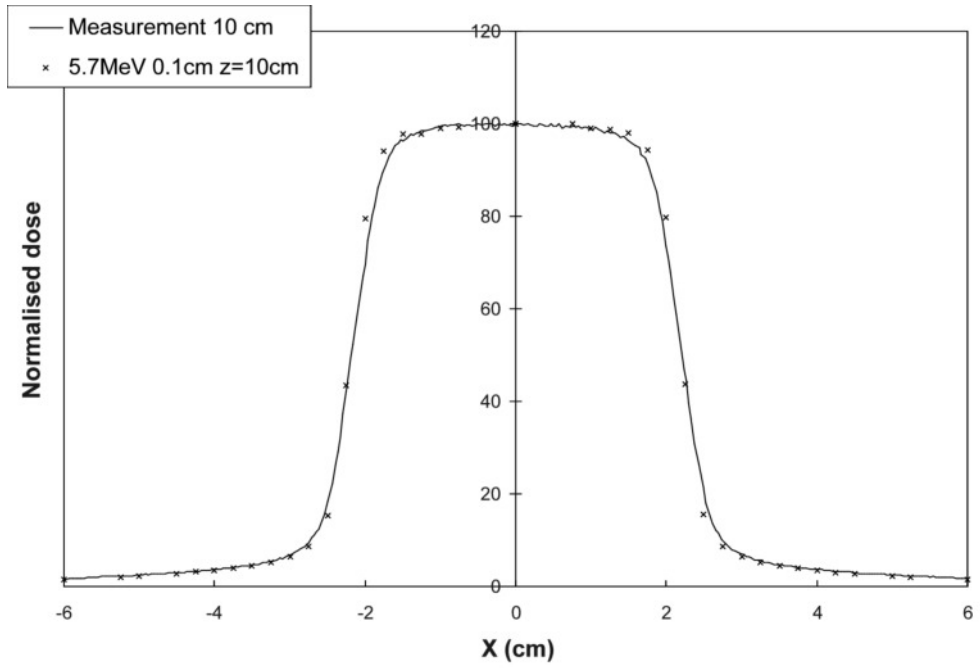

(c)

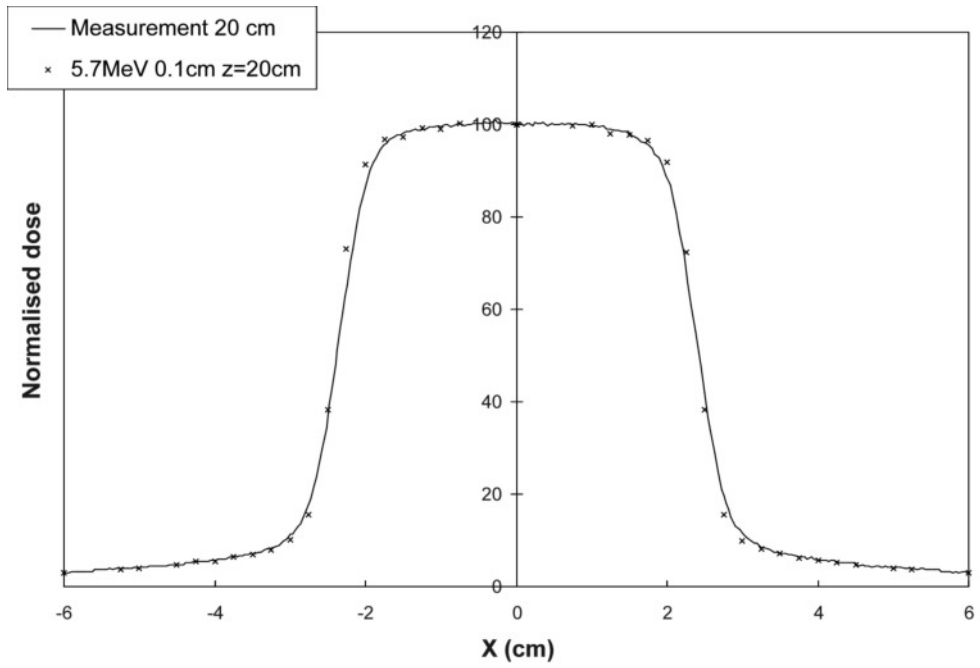

(d)

Figure 5: Dose profile for 4x4 cm^2 field size in water phantom at a) 1.5 cm, b) 5 cm, c) 10 cm, d) 20 cm depth. Solid line measured (CC13) and discrete points simulated. The uncertainties of the simulated values (+-1SE) are represented by the size of the data points.

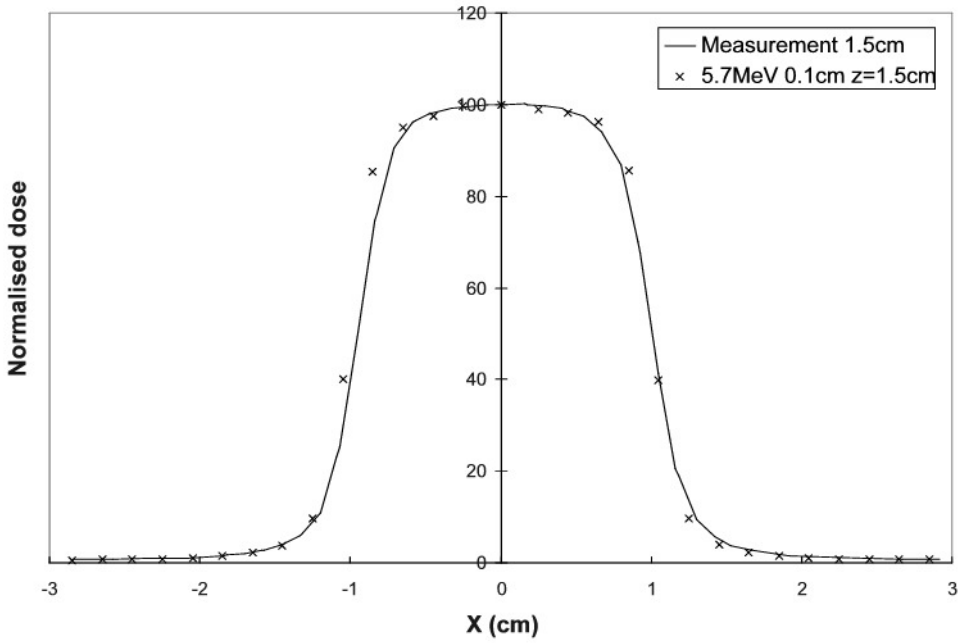
Measurement 1.5cm
5.7MeV 0.1cm z=1.5cm
Normalised dose
X (cm)
120
100
80
60
40
20
0
-3
-2
-1
0
1
2
3

(a)

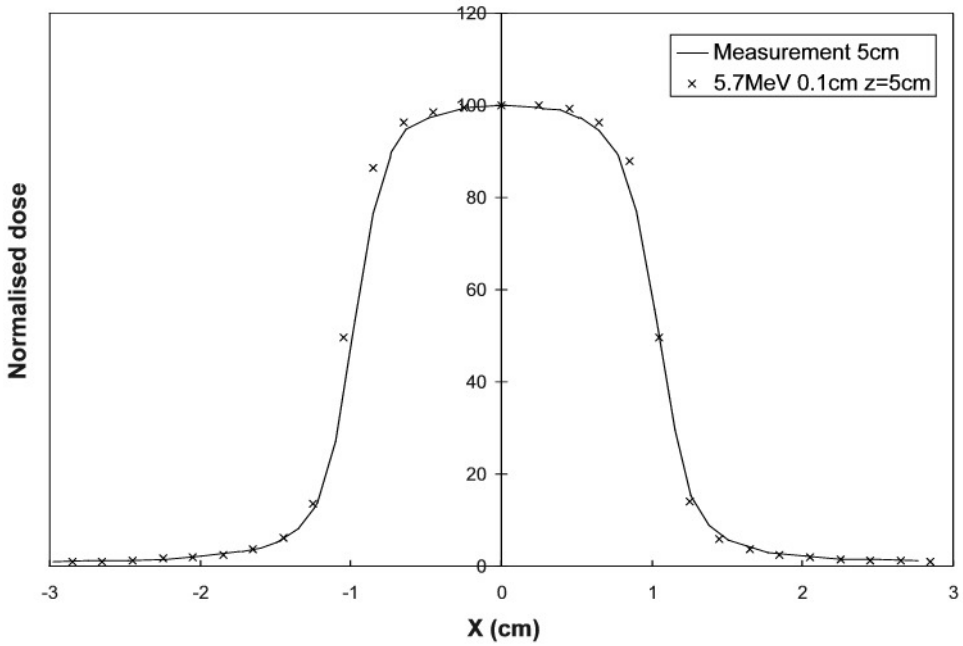
Measurement 5cm
5.7MeV 0.1cm z=5cm
Normalised dose
X (cm)
120
100
80
60
40
20
0
-3
-2
-1
0
1
2
3

(b)

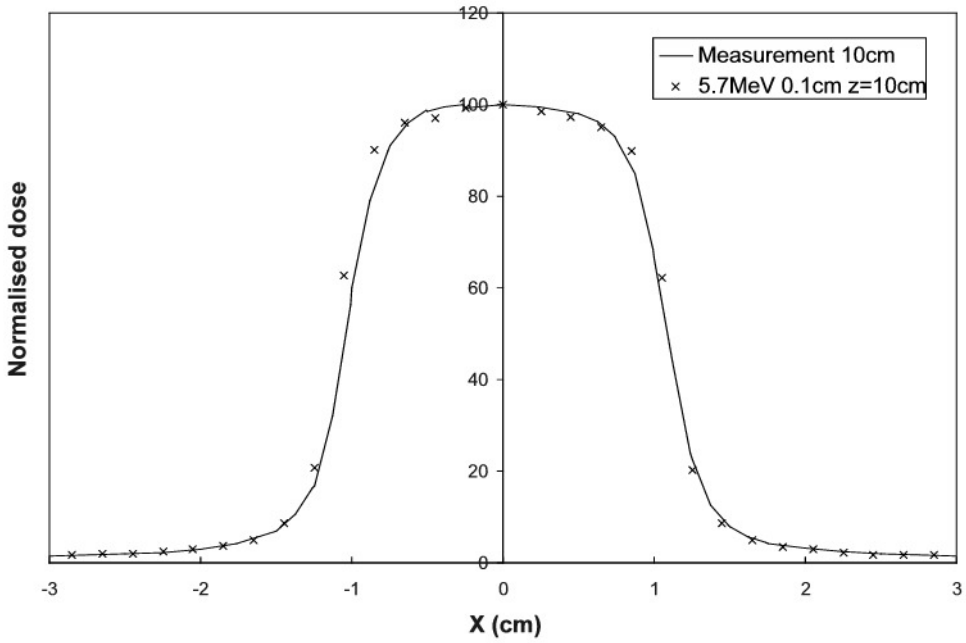

(c)

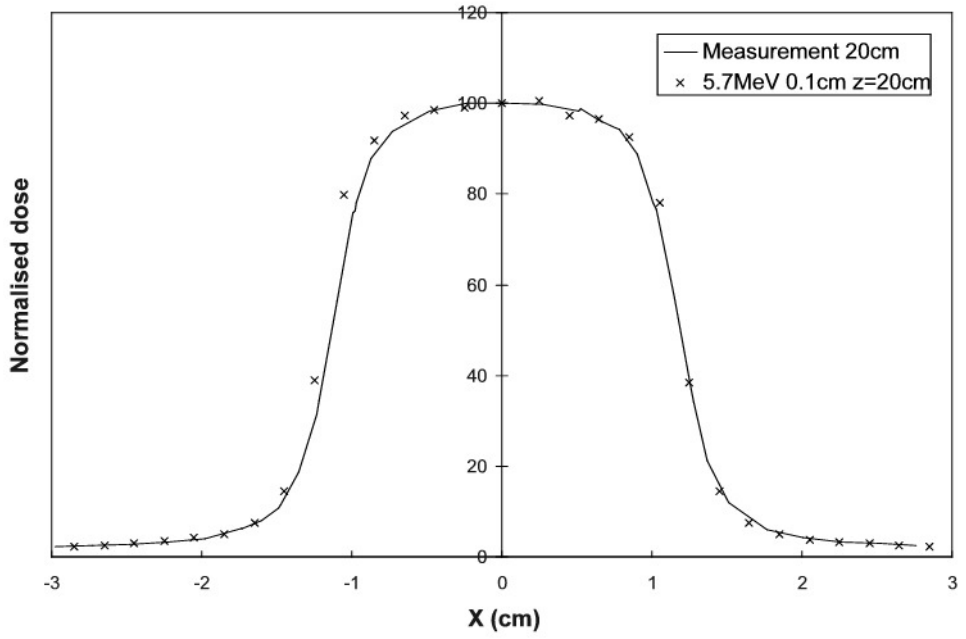

(d)

Figure 6: Dose profile for 2x2 cm^2 field size in water phantom at a) 1.5 cm, b) 5 cm, c) 10 cm, d) 20 cm depth. Solid line measured (pin-point, steel electrode) and discrete points simulated. The uncertainties of the simulated values (+-1SE) are represented by the size of the data points.

3.2.2 Y-direction Dose Profiles

Dose profiles in y-direction were analysed visually for a 10x10 cm^2 and a 20x20 cm^2 field. The comparison between measured and simulated data are shown in Figures 7 to 8.

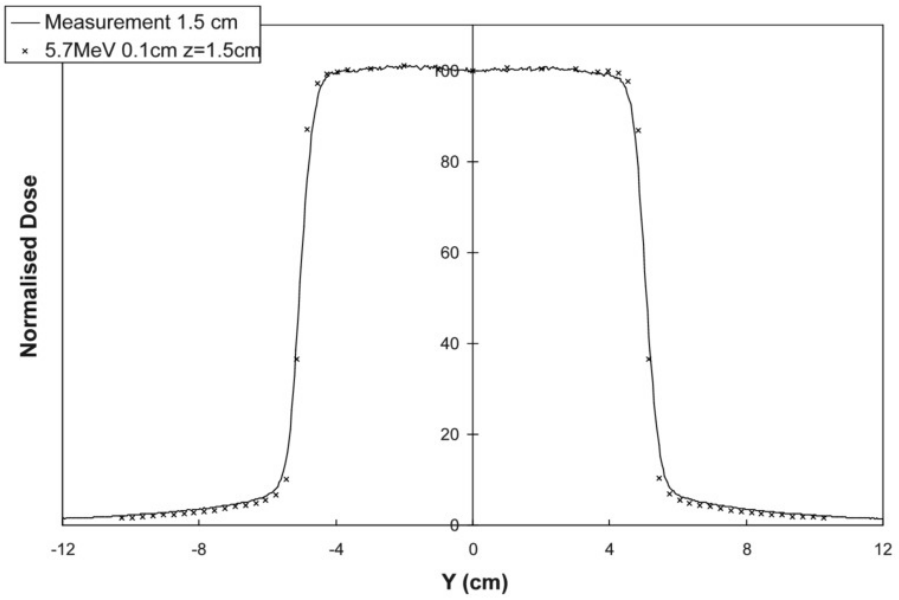

(a)

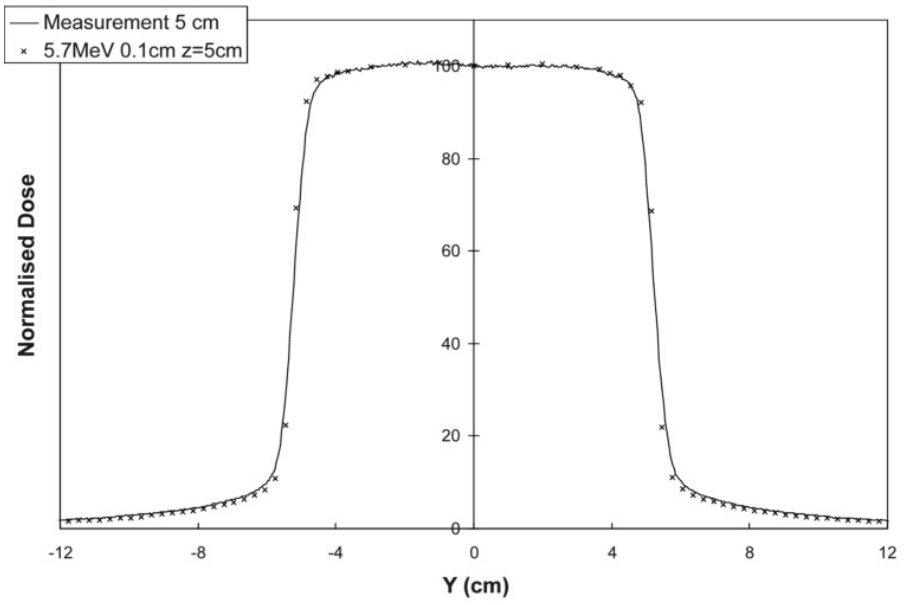

(b)

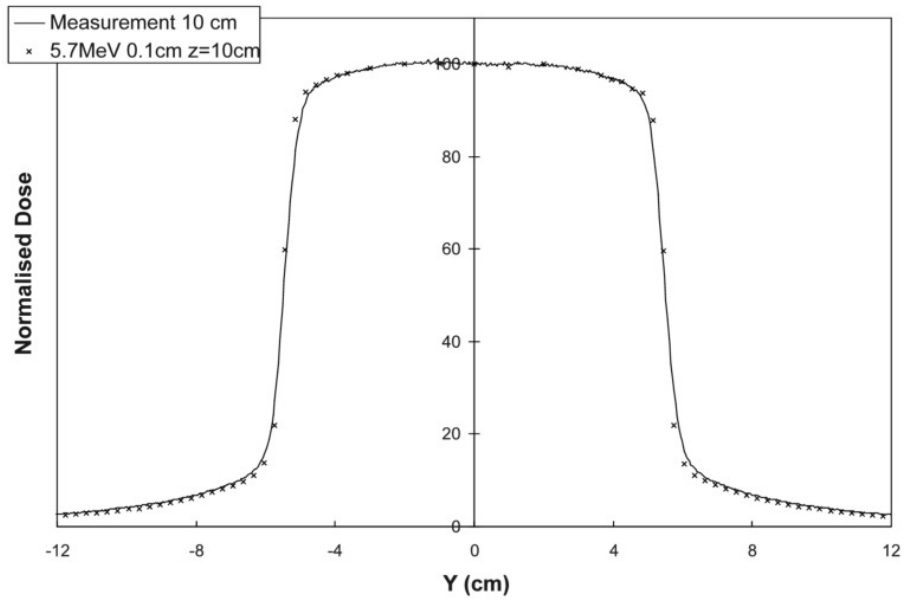

(c)

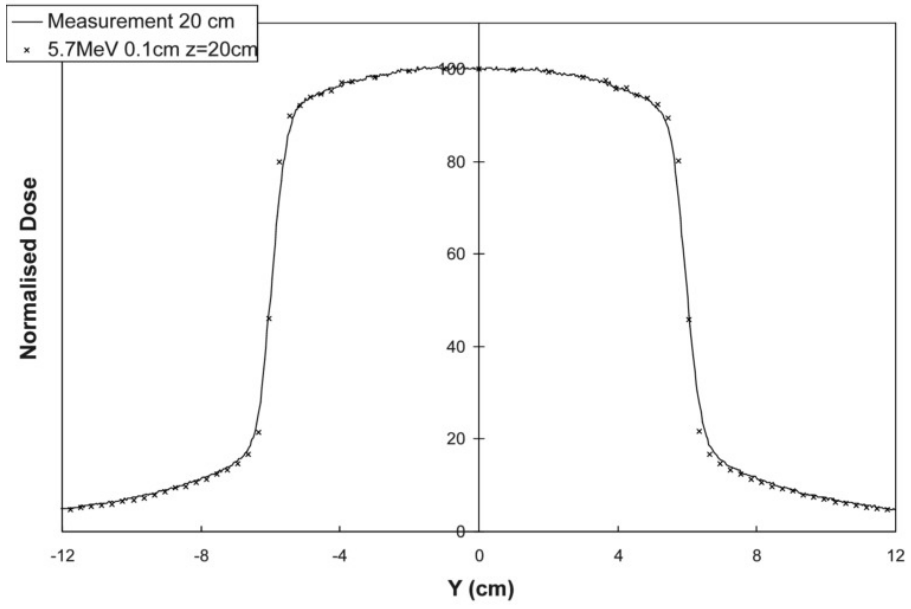

(d)

Figure 7: Y-direction dose profile for 10x10 cm^2 field size in water phantom at a) 1.5 cm, b) 5 cm, c) 10 cm, d) 20 cm depth. Solid line measured (CC13) and discrete points simulated. The uncertainties of the simulated values (+-1SE) are represented by the size of the data points.

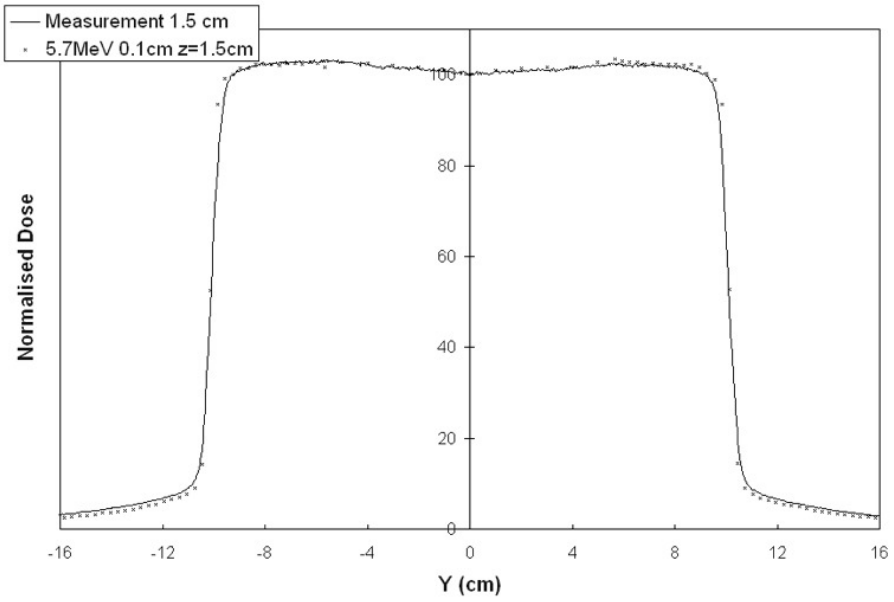
Measurement 1.5 cm
5.7MeV 0.1cm z=1.5cm
Normalised Dose
Y (cm)
0
20
40
60
80
100
-16
-12
-8
-4
0
4
8
12
16

(a)

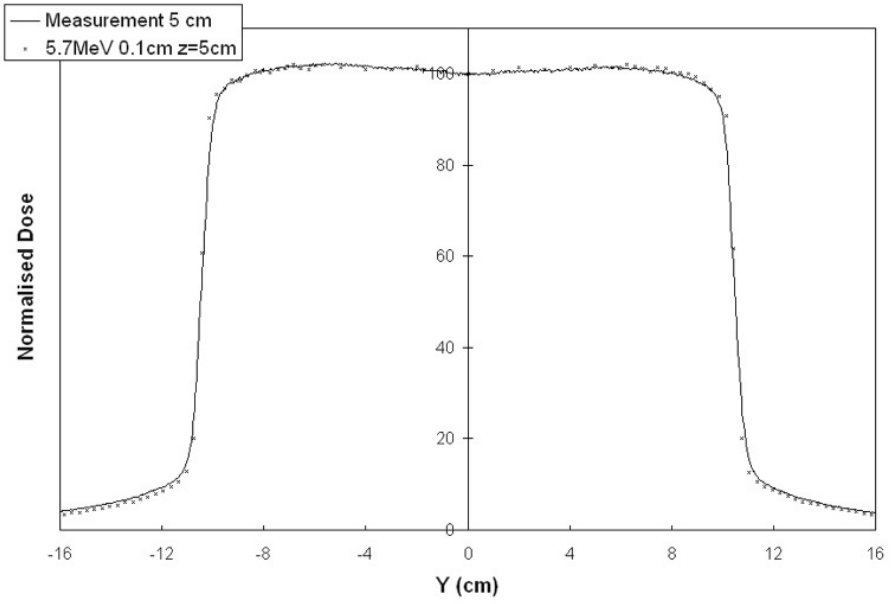
Measurement 5 cm
5.7MeV 0.1cm z=5cm
Normalised Dose
Y (cm)
0
20
40
60
80
100
-16
-12
-8
-4
0
4
8
12
16

(b)

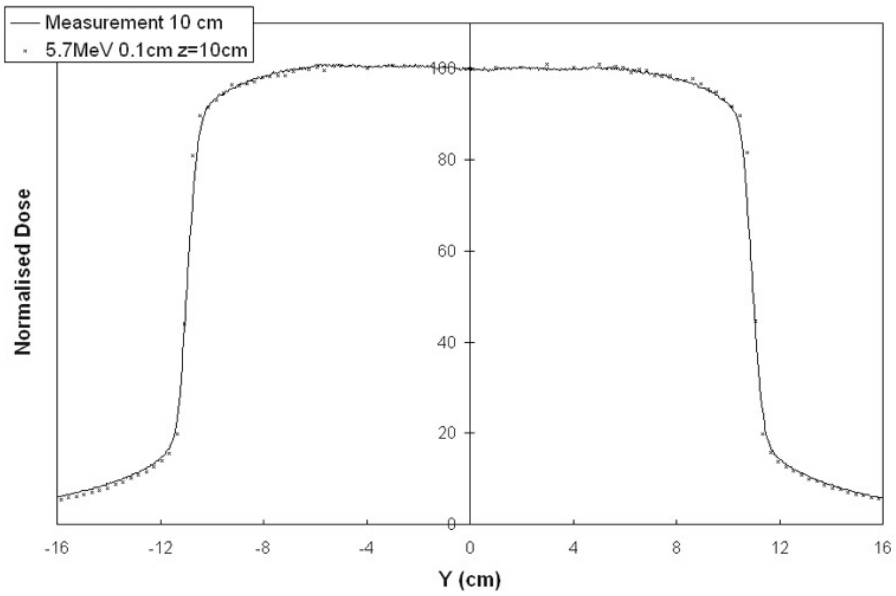

(c)

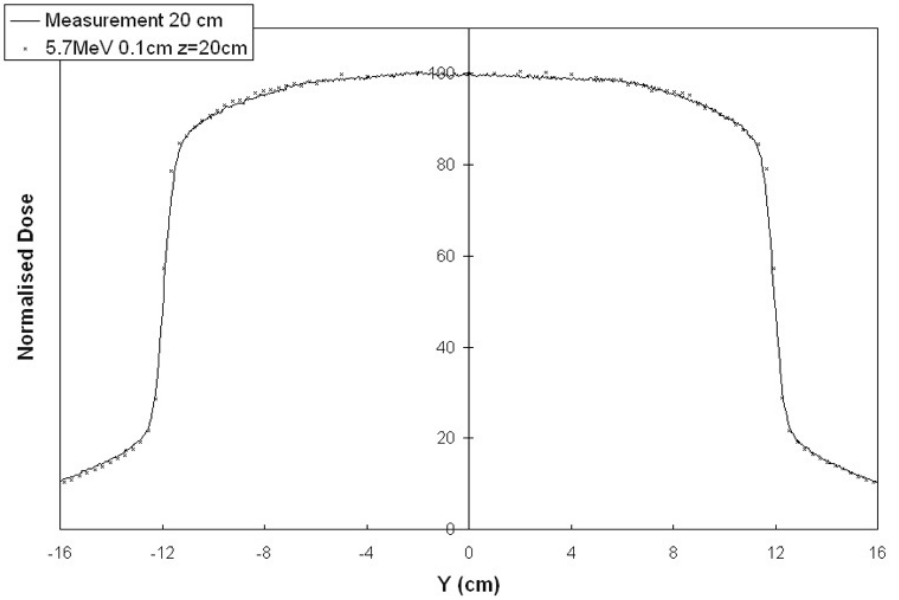

(d)

Figure 8: Y-direction dose profile for 20x20 cm^2 field size in water phantom at a) 1.5 cm, b) 5 cm, c) 10 cm, d) 20 cm depth. Solid line measured (CC13) and discrete points simulated. The uncertainty of the simulated values (+-1SE) are represented by the size of the data points.

3.2.3 Depth Dose Curves

The depth dose verification curves for parameter set [5.7 MeV 0.1 cm] are shown in Figures 9 to 13. The dose has been normalised (100%) to dose at 10 cm depth, taken from a fifth grade polynomial fitted to the simulated data points between the depths 5 and 20 cm. In all cases the simulated data points do not deviate more than 1% (of the dose in dose max) from the measured data between the depth of dose max and 25 cm, except for in the case of 2x2 cm^2 field, in which the deviation at dose maximum is 2.5% of the dose at dose maximum.

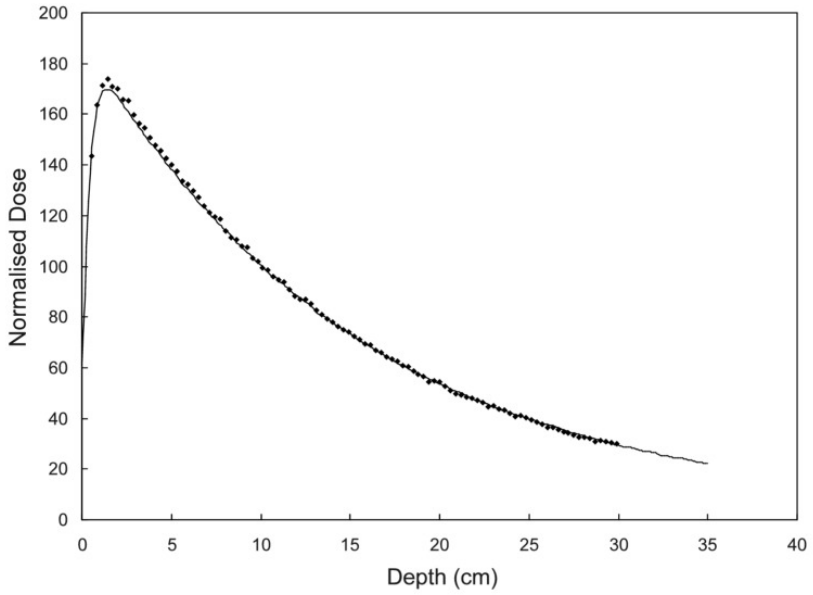

Figure 9: Depth dose curve for 2x2 cm^2 field size in water phantom. Solid line measured (pin-point, steel electrode) and discrete points simulated. The uncertainties of the simulated values (+-1SE) are represented by the size of the data points.

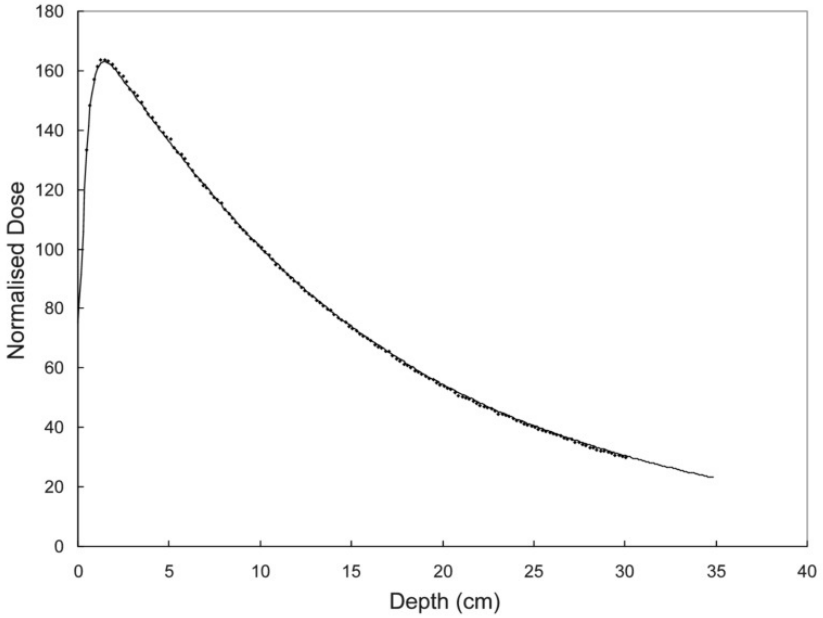

Figure 10: Depth dose curve for 4x4 cm^2 field size in water phantom. Solid line measured (CC13) and discrete points simulated. The uncertainties of the simulated values (+-1SE) are represented by the size of the data points.

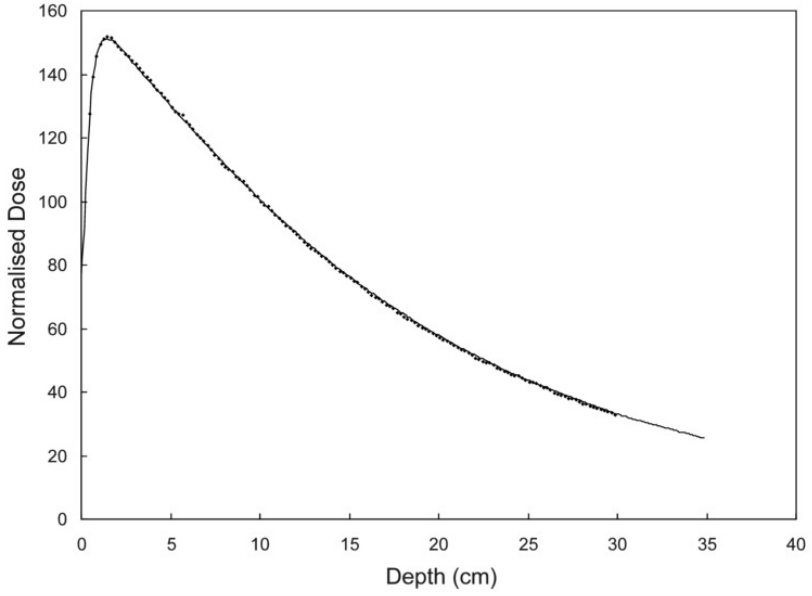

Figure 11: Depth dose curve for 10x10 cm^2 field size in water phantom. Solid line measured (CC13) and discrete points simulated. The uncertainties of the simulated values (+-1SE) are represented by the size of the data points.

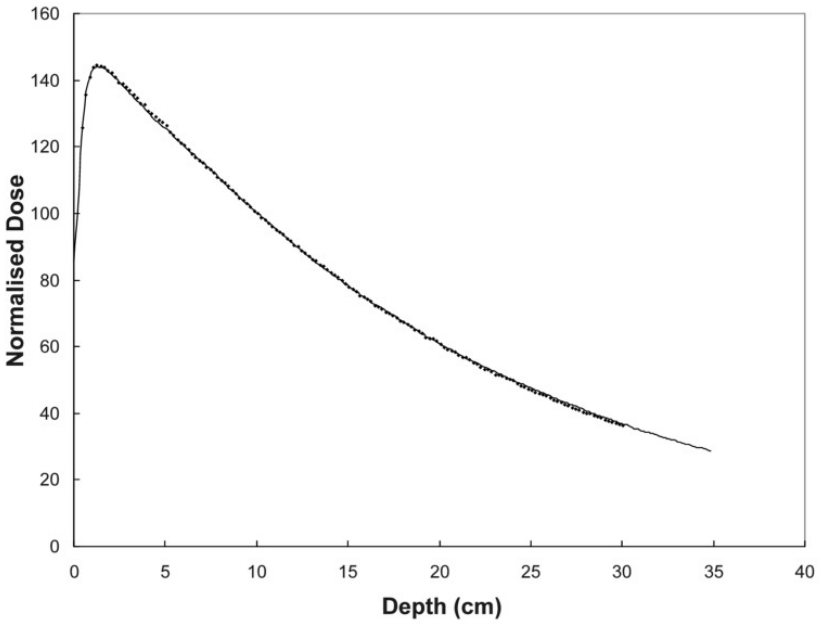

Figure 12: Depth dose curve for 20x20 cm^2 field size in water phantom. Solid line measured (CC13) and discrete points simulated. The uncertainties of the simulated values (+-1SE) are represented by the size of the data points.

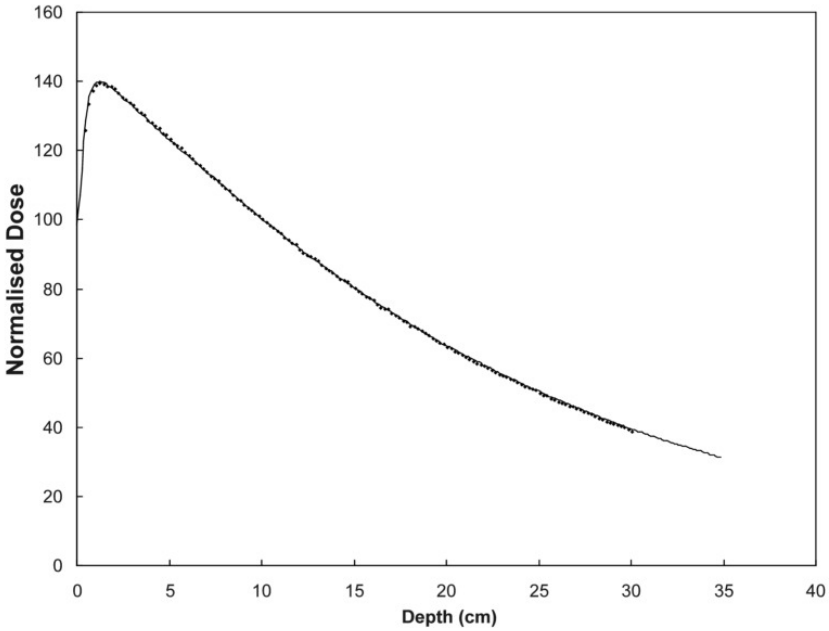

Figure 13: Depth dose curve for 40x40 cm^2 field size in water phantom. Solid line measured (CC13) and discrete points simulated. The uncertainties of the simulated values (+-1SE) are represented by the size of the data points.

3.2.4 Output Factors

The results from the output-factor determination are presented in Table 1 and 2. The results from calculations based on simulated doses taken from polynomial fit of the simulated depth dose curve are presented in Table 1 and the results from calculations based on simulated doses taken from single voxels are presented in Table 2. For comparison the measured output factors are presented as well. The differences between measured and calculated values normalised to the measured value are shown in column 3. In Table 2 the uncertainty of the normalised difference between measured and simulated output factors is presented. It is seen from Table 1 that the simulated output factors do not deviate more than 2.3% from measured output factors. For field sizes smaller than 20x20 cm^2 the deviation is less than 1.65%.

Table 1: Table of results from output-factor calculations based on doses from polynomial fits of depth dose curves. First column specifies field size ratio (symmetrical fields). Column 1; measured output factors. Column 2; simulated output factors. Column 3; Difference between simulated and measured ratios in percent of the measured ratio.

	1	**2**	**3**
(cm^2/cm^2)	**Meas OF**	**Sim OF**	**[sim-meas]/meas*100**
2x2/10x10	0.79	0.80	0.16
4x4/10x10	0.86	0.87	0.93
10x10/10x10	1	1	0
20x20/10x10	1.10	1.08	-1.65
40x40/10x10	1.19	1.16	-2.30
x4y20/10x10	0.94	0.94	-0.02
x20y4/10x10	0.92	0.93	0.59

Table 2: Table of results from output-factor calculations based on doses taken from single voxels. First column specifies field size ratio (symmetrical fields). Column 1; measured output factors. Column 2; simulated output factors. Column 3; Difference between simulated and measured ratios in percent of the measured ratio. Column 4; Uncertainty (expressed as the standard error) in the quantity given in column 3.

	1	**2**	**3**	**4**
(cm^2/cm^2)	**Meas OF**	**Sim OF (voxel)**	**[sim-meas]/meas*100**	**SE of column 3**
2x2/10x10	0.79	0.79	-0.32	1.42
4x4/10x10	0.86	0.87	1.37	0.59
10x10/10x10	1	1	0	-
20x20/10x10	1.10	1.10	-0.60	0.56
40x40/10x10	1.19	1.16	-2.17	0.54
x4y20/10x10	0.94	0.94	-0.02	0.53
x20y4/10x10	0.92	0.93	0.41	0.54

4 Conclusion

The final parameter set for modelling of the Varian Clinac iX linear accelerator was chosen to be 5.7 MeV monoenergetic electrons hitting the target normally with a gaussian spatial distribution of FWHM 0.1 cm. All simulated data points in the depth dose curves deviated less than 1% of the dose at dose maximum from the measured data, except for the data points around dose max in a 2x2 cm^2 field. The criteria of maximum 1% (of the dose in dose maximum) deviation was further fullfilled in all profiles, except for those at 1.5 cm depth, where the maximum deviation was 1.7%, 1.4% and 1.5% for 10x10, 20x20 and 40x40 cm^2 field sizes respectively.

The simulated output factors for fields of length smaller than 20 cm could be assessed to within 1.65% of the measured output factors.

References

[1] B. Walters D.W.O. Rogers and I. Kawrakow. Beamnrc users manual. *NRC Report PIRS-0509(A)revK*, 2009.

[2] F. Hasenbalg et. al. Vmc++ versus beamnrc: A comparison of simulated linear accelerator heads for photon beams. *Med. Phys.*, 35, 1521-1531 (2008).

[3] Daryoush Sheikh-Bagheri and D.W.O Rogers. Sensitivity of megavoltage photon beam monte carlo simulations to electron beam and other parameters. *Med. Phys.*, 29, 379-390 (2002).

[4] J. H. Hubbell and S. M. Seltzer. Tables of x-ray mass attenuation coefficients and mass energy-absorption coefficients 1 kev to 20 mev for elements z=1 to 92 and 48 additional substances of dosimetric interest. *Technical Report NISTIR 5632*, NIST, Gaithersburg, MD, 1995.

[5] B. R. B. Walters *et. al.* History by history statistical estimators in the beam code system. *Med. Phys.*, 29, 2745-2752 (2002).